Plasmon mode transformation in modulated-index metal-dielectric slot waveguides

Ning-Ning Feng* and Luca Dal Negro

Department of Electrical and Computer Engineering, Boston University, 8 Saint Mary's Street, Boston, Massachusetts, 02215-2421, USA
**Corresponding author: fengn@bu.edu*

Received May 31, 2007; revised September 5, 2007; accepted September 9, 2007;
posted September 26, 2007 (Doc. ID 83614); published October 18, 2007

The concept of adiabatic mode transformation between silicon waveguide and surface plasmon-polariton modes in subwavelength metal-dielectric slots is investigated. The mode transformer consists of a modulated-index slot region, which is bound by two metal slabs. Using the design scheme, we will show that the optical dispersion of a modulated-index metal slot waveguide can be engineered well above the silicon light-line on a large wavelength region, allowing direct phase-matching between surface plasmon polaritons and traditional waveguide modes. Based on full-field, finite difference simulations, we demonstrate that reversible mode conversion can be achieved within submicrometer length scales. © 2007 Optical Society of America

OCIS codes: 130.2790, 130.3120, 240.6680.

Near-field coupling and resonant excitation of surface plasmon polaritons (SPPs) in metal nanoparticle arrays and metal slot waveguide structures have recently suggested fascinating strategies for nanoscale guiding and control of subwavelength fields on planar chips [1–3]. In particular, unique nanoscale optical devices such as plasmonic waveguides [4], enhanced nanodetectors–emitters [5], and optical nanoantennas [6,7] have been recently demonstrated, implying a successful convergence of optics and electronics at the nanoscale. However, it has been recently shown that a fundamental trade-off exists between the spatial localization of SPP modes and propagation losses [8–10], which can only be alleviated by carefully designed metal-dielectric structures. It can be envisioned that reliable strategies for SPP to waveguide mode transformation can lead to the effective interrogation and control of localized optical fields, which are central for a variety of emerging applications such as local field and nanofluidics sensing, plasmon-enhanced input–output local field injectors–extractors, and sharp bending elements based on the SPP confinement of nanoscale optical fields. However, it is well known that localized SPP waves cannot be directly excited by transverse plane waves because of a fundamental momentum mismatch [11]. Recently, it has been shown that a standard adiabatic taper can efficiently launch subwavelength localized SPPs at 1.55 μm when coupled to metal slot waveguides with a high index dielectric medium (silicon) filling the slot region [12].

In this Letter, we propose to investigate the concept of wide-band, reversible mode conversion between conventional silicon waveguide modes and SPP waves. By engineering the full band-dispersion diagram of modulated-index metal-dielectric slot waveguides, we demonstrate that efficient phase-matching and mode transformation between SPPs and traditional waveguide modes can be achieved on a large spectral range.

A schematic of the proposed SPPs mode transformer is shown in Figs. 1(a) and 1(b). The proposed structure consists of two conventional silicon waveguides, which are adiabatically tapered inside the slot region of a metal slot waveguide structure with a modulated-index profile in the slot region. A thin SiO_2 gap region (refractive index $n_{SiO_2}=1.46$) separates the metal (Ag) from the high index (Si, $n_{Si}=3.5$) waveguide core. The geometrical parameters of the mode transformer are $w_d=450$ nm, $h=300$ nm, $w_t=200$ and 150 nm, $w_s=100$ nm, $L_t=500$ nm, and $L_s=400$ nm. These parameters have been on the basis of our previous work [10], to provide minimum propagation losses.

Our numerical study is based on the full-vector finite-difference (FD) approach [13]. The optical response of Ag has been modeled using the tabulated

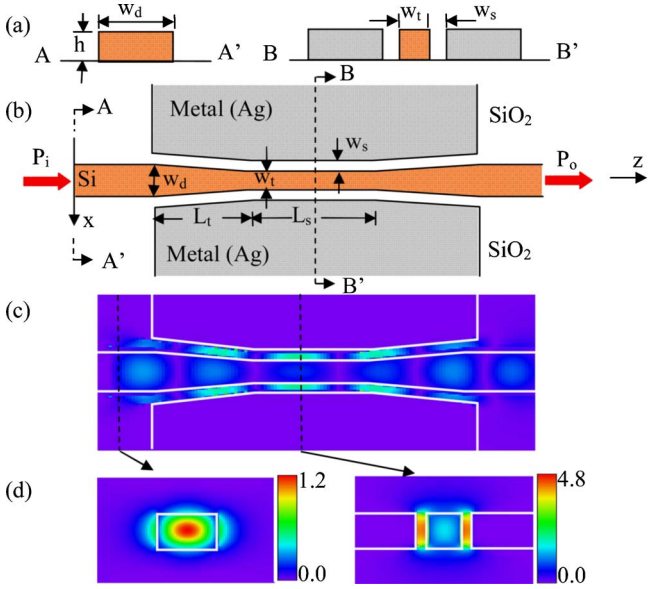

Fig. 1. (Color online) Schematics of the proposed SPP mode transformer: (a) cross sections (z cut) of the structure at different locations, (b) top view of the structure (y cut), (c) top-view field distribution (y cut at the center of the waveguide) simulated by 3D FDTD, and (d) cross-section views of the field at the launch position and at the center of the structure.

dielectric function values as in [14]. In Fig. 2 we show the dispersion diagram at the center of the transformer [across the B–B′ cut in Fig. 1(a)] calculated for different gap widths w_s. Figure 2 clearly illustrates the substantial difference between standard metal slots and modulated-index slot structures. The dispersion diagrams for these two types of structures are quite different, even when the gap width is as small as $w_s=20$ nm (Fig. 2, green triangles). Our previous work [10] has shown that the electric field can be strongly localized inside the subwavelength, low-index gaps in modulated-index slot waveguide structures. This effect is due to the significant reduction of the SPPs mode effective index and leads to a dramatic modification in the dispersion diagram of modulated-index slot waveguides with respect to traditional slot structures. In particular, as shown in Fig. 2, it is possible to engineer the band dispersion of modulated-index metal slot waveguides entirely above the Si light line (Fig. 2, diamonds) on a large wavelength region, allowing broadband phase matching between SPPs and traditional waveguide modes. On the other hand, we notice that for structures without the low-index gap ($w_s=0$ nm), the dispersion curve (Fig. 2, inverse triangles) lies above the Si light line within the wavelength range of 1.5–2.8 μm. This implies that structures without a low-index gap cannot operate the transformation from regular Si waveguide modes to SPPs for wavelengths that are shorter than 1.5 μm. On the other hand, when $w_s>0$ nm (modulated-index waveguides case), the dispersion diagram lies entirely above the Si light line for wavelengths that are shorter than the cutoff wavelength, ~2 μm in our simulation conditions. However, we notice that the plasmonic waveguide cutoff wavelength can be shifted to even longer wavelengths, depending on the refractive index and the width of the gap and cladding regions. These characteristics of the modulated-index slot transformers open new possibilities for direct excitation of SPP modes by regular Si waveguides over a broad wavelength spectrum, ranging from the bandgap absorption wavelength (~1.1 μm for Si) to the cutoff wavelength of the plasmonic waveguide [10].

Figure 3 shows the calculated optical transmission of a modulated-index structure as a function of the low-index gap width w_s. In this case, the simulation of the optical transmission is performed using a 3D finite-difference time domain (FDTD) approach (FullWave, Roft Design Inc.). From Fig. 3 we notice that in the limit of large low-index gap width, the structure of our proposed transformer is reduced to regular waveguide taper pairs. In this limit, the optical transmission approaches the values obtained for regular waveguide taper pairs, which are ~39% and 56% in the case of two taper pairs with $w_t=150$ and $w_t=200$ nm, limited by radiation losses. On the other hand, by reducing the gap width of modulated-index metal slots, the transmitted optical power for the TE polarization is strongly enhanced due to the resonant coupling with surface-plasmon modes. Interestingly, we observe that at intermediate gap widths the TE polarized transmission is strongly reduced, and it is almost extinguished for a gap width of ~0.4 μm. This behavior is the result of the enhanced, plasmon-mediated optical losses discussed in our previous work [10]. In fact, we showed that when the plasmon-waveguide effective index matches the index of the cladding region, which occurs at a gap width of 0.4 μm for the current design, the optical power leaks out from the wave-guiding region in the form of free-space radiation modes as well as propagating SPP modes excited at the top–bottom metal surfaces, as shown in the inset of Fig. 3. However, a further decrease of the gap width leads to a substantial increase in the slot waveguide effective index, which results in the efficient excitation (for TE polarization) of plasmonic modes confined in the guiding region. As

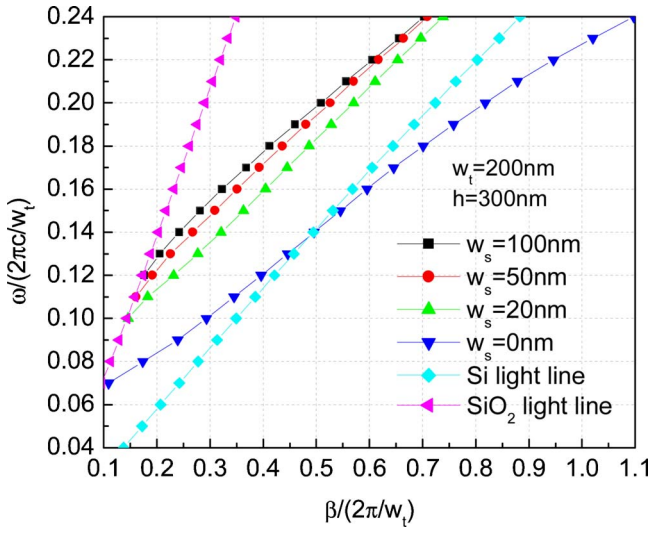

Fig. 2. (Color online) Dispersion relations of the metal slot transformer calculated at the B–B′ cut as shown in Fig. 1(a) for different gap distances w_s. The SiO_2 gap region separates the metal (Ag) from the high index (Si) waveguide core.

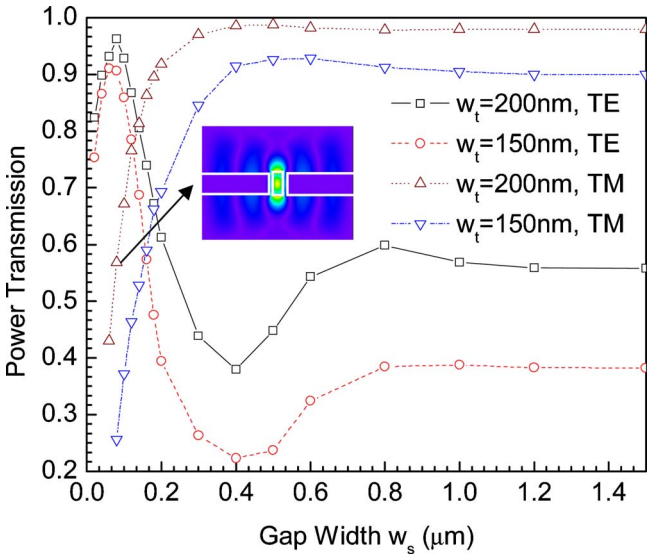

Fig. 3. (Color online) SPP mode transformer calculated optical power transmission versus the low-index gap width for TE and TM polarizations. The inset shows the electric field profile for TM polarization corresponding to a gap width of 100 nm.

a result, the optical power transmission is enhanced up to 91% and 95% for modulated-index transformers with $w_t = 150$ and $w_t = 200$ nm, respectively (Fig. 3). The sharp decrease in the optical transmission for gap widths smaller than 150 nm is due to the enhanced optical absorption of strongly localized SPP modes, and illustrates in very clear terms the fundamental trade-off between plasmon localization and optical losses, which we have discussed in [10]. The top-view and cross-sectional view of the FDTD calculated optical field profiles in the waveguide and inside the transformer are shown in Figs. 1(c) and 1(d), respectively. Figure 1(d), which has also been obtained using the full-vector FD approach [10], clearly indicates that an SPP mode has been excited in the central section of the mode transformer. The field is localized inside subwavelength low-index gaps (100 nm) with ~16 times field intensity enhancement compared to a normal Si waveguide mode. The plasmonic nature of the mode shown in Fig. 1(d) is highlighted by noticing that the optical transmission enhancement can only be achieved in the case of TE excitation. In fact, the calculated transmission for the TM polarization has been found to be strongly suppressed, since SPP waves will propagate bound to the top–bottom metal interfaces (Fig. 3, inset), resulting in strong radiation and insertion losses.

In Fig. 4 we show the behavior of the calculated power transmission versus the taper end width w_t [Fig. 4(a)], where the results are compared between normal Si waveguide tapers and the proposed SPP mode transformers (waveguide tapers with metal slots). It is found that there is an optimal taper end width for a fixed taper length, which yields a maximum power transmission of the metal slot taper. This effect is again a direct consequence of the fundamental trade-off between metal losses and plasmon localization [10]. However, our analysis reveals that the SPPs-enhanced optical transmission is larger for the tapers with smaller end width w_t in the region where a large suppression of the optical transmission is observed for a Si waveguide taper without metal slots. For tapers with larger end widths (keeping the low-index gap width constant), the power transmission decreases because of the increased effective index of the SPP waveguide, which induces larger propagation losses [10]. The FDTD-calculated optical transmission spectra of the transformer are shown in Fig. 4(b). The data demonstrate that the SPPs-enhanced power transmission is indeed a wide-band phenomenon, and that reversible mode conversion can be achieved within submicrometer length scales with insertion losses lower than 0.2 dB. Considering propagation losses of 0.1 dB/μm [10], we can deduce that for $L \approx 1$ μm long coupler the coupling losses (waveguide to SPP mode) are less than 0.1 dB. Finally, it is worthwhile addressing the effect of the taper length. We have found that there is an optimum taper length due to the interplay of the taper losses and propagation losses, in agreement with the results discussed in [12]. The taper losses are dominant for the shorter taper lengths, and the propagation losses are dominant for the longer device lengths, due to metal absorption. Accordingly, in our design study we selected a taper length of $L_t = 500$ nm to achieve the lowest insertion losses.

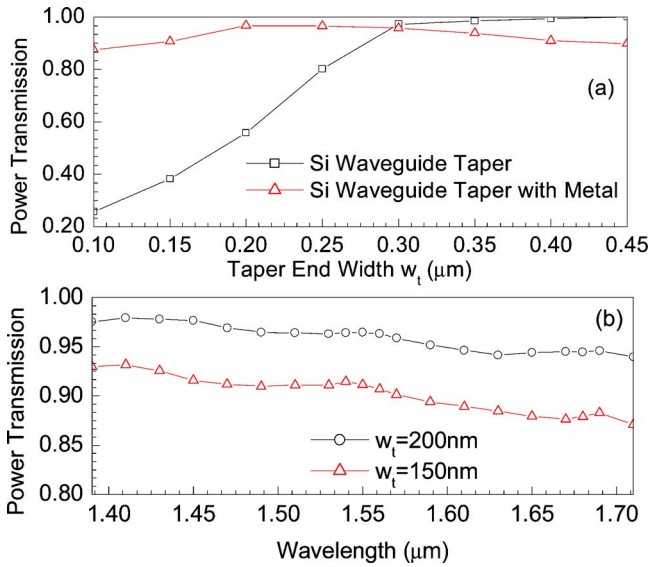

Fig. 4. (Color online) Calculated optical power transmission versus (a) taper end width w_t and (b) operating wavelength for normal Si waveguide tapers and Si waveguide tapers with metal slots (SPP transformer).

In conclusion, based on full-vector FD analysis, we have designed a modulated-index metal-slot waveguide transformer. We have shown that its optical dispersion can be engineered entirely above the Si light line on a very large wavelength region, allowing efficient direct phase matching and mode transformation between SPPs and traditional waveguide modes.

References

1. W. L. Barnes, A. Dereus, and T. W. Ebbesen, Nature **424**, 824 (2003).
2. E. Ozbay, Science **311**, 189 (2006).
3. R. Zia, J. A. Schuller, and M. L. Brongersma, Mater. Today **9**, 27 (2006).
4. S. A. Maier, M. L. Brongersma, P. G. Kik, S. Meltzer, A. A. G. Requicha, and H. A. Atwater, Adv. Mater. (Weinheim, Ger.) **13**, 1501 (2001).
5. Z. Yu, G. Veronis, S. Fan, and M. L. Brongersma, Appl. Phys. Lett. **89**, 151116 (2006).
6. K. B. Crozier, S. Sundaramurthy, G. S. Kino, and C. F. Quate, J. Appl. Phys. **94**, 4632 (2003).
7. N. Anderson, A. Bouhelier, and L. Novotny, J. Opt. A, Pure Appl. Opt. **8**, S227 (2006).
8. Z. Rashid, M. D. Selker, P. B. Catrysse, and M. L. Brongersma, J. Opt. Soc. Am. A **21**, 2442 (2004).
9. J. A. Dionne, L. A. Sweatlock, H. A. Atwater, and A. Polman, Phys. Rev. B **73**, 035407 (2006).
10. N. N. Feng, M. L. Brongersma, and L. Dal Negro, IEEE J. Quantum Electron. **43**, 479 (2007).
11. H. Raether, *Surface Plasmons on Smooth and Rough Surfaces and on Gratings* (Springer-Verlag, 1988).
12. L. Chen, J. Shakya, and M. Lipson, Opt. Lett. **31**, 2133 (2006).
13. N. N. Feng, G. R. Zhou, C. L. Xu, and W. P. Huang, J. Lightwave Technol. **20**, 1976 (2002).
14. E. D. Palik, ed., *Handbook of Optical Constants of Solids* (Academic, 1985).